CuKα radiation and Fourier-transform infrared (FTIR) spectroscopy (Spectrum One, Perkin-Elmer Inc., MA, USA) were performed. The results are shown in Fig. 1. In Figs. 1(a) and (b), both XRD profiles showed highly crystalline HAp, and no other calcium phosphate phases could be detected. In the FTIR spectrum of HAp calcined with $Ca(OH)_2$ (Fig. 1(d)), no peaks due to stretching of OH in $Ca(OH)_2$ were observed at 3640 cm^{-1}, indicating complete removal of $Ca(OH)_2$. Bonel *et al.* prepared calcium-rich apatites with a Ca/P molar ratio above 1.67 by heating a mixture of stoichiometric HAp [$Ca_{10}(PO_4)_6(OH)_2$; Ca/P = 1.67] and $CaCO_3$ in moist air at 1000°C for 10 days, and identified additional OH IR bands at 3544, 745, 715, and 680 cm^{-1} [15]. In the present study, although the additional band at 3544 cm^{-1} was observed, the Ca/P ratio of the HAp calcined with $Ca(OH)_2$ was 1.58 (1.56 in the case of the HAp calcined without $Ca(OH)_2$). These results suggest that calcination with $Ca(OH)_2$ led to the formation of a calcium-rich apatite phase only on the outermost surface, presumably because the conditions (temperature, time, composition of atmosphere) were too mild for a reaction between HAp and $Ca(OH)_2$. It is worth pointing out that the calcium-rich carbonate-substituted HAp had improved mechanical and biological properties compared to stoichiometric HAp [16].

Fig. 2 shows SEM and TEM micrographs of HAp crystals calcined with or without $Ca(OH)_2$. As seen in the lower magnification images in Figs. 2 (a) and (b), the crystal size ranged from 30 to 80 nm, irrespective of the presence or absence of $Ca(OH)_2$. The higher magnification TEM image of a particle calcined with $Ca(OH)_2$ and its electron diffraction pattern (Figs. 2 (c) and (d), respectively) confirmed that the particle was a single HAp crystal with an irregular spherical morphology. The size of HAp crystals dispersed in ethanol was measured by DLS (Fig. 3). In the case of calcination without

$Ca(OH)_2$, the mean size was about 600 nm, which indicates the formation of agglomerates of sintered HAp polycrystals. In the case of calcination with $Ca(OH)_2$, the size of particles dispersed in ethanol ranged from 80 to 130 nm, which is close to the primary crystallite size (30 to 80 nm) determined by electron micrographs. This indicates that sintering between the HAp nanocrystals can be mostly prevented by interspersing $Ca(OH)_2$ between the crystals prior to calcination.

However, the size of the dispersed crystals was slightly larger than that of the primary particles. This is should be because HAp particles have both anionic and cationic surfaces, and hence, tend to flocculate in aqueous media. The particle size measurements indicate that these agglomerates that formed during interspersion of the $Ca(OH)_2$ contained several HAp particles each. Thus, poly(acrylic acid) (PAA) was added as a deflocculant before the addition of $Ca(OH)_2$. PAA can adsorb on the HAp surfaces [17, 18], and thus, act as a polymeric dispersant. The addition of calcium ions into an aqueous PAA solution induces a rapid precipitation of poly(acrylic acid calcium salt) (PAA-Ca). Thus, when calcium ions are added to the PAA-stabilized HAp dispersion, PAA-Ca precipitates onto the surface of the HAp particles, and presumably acts as an anti-sintering agent. In the present study, an amount of PAA (Sigma-Aldrich Co.; weight-average molecular weight: 15,000), approximately equal in weight to the HAp particles, was added under alkaline conditions (initial pH: 10). An excess amount of calcium ions were added to the dispersion in the form of a saturated aqueous $Ca(OH)_2$ solution ($Ca(OH)_2$/COOH in PAA = 1/1 molar ratio). The resultant HAp/PAA-Ca mixture was calcined in the manner described above, and then washed to remove CaO, the product of thermal decomposition of PAA-Ca. The resultant HAp crystals are shown in Fig. 4. The size of the HAp crystals dispersed in ethanol (40 to 70

nm) corresponded to that of the primary crystallites (30 to 80 nm), which indicates that HAp nanocrystals calcined with PAA-Ca can be dispersed as single crystals. IR spectrum and XRD pattern of the HAp single crystals calcined with PAA-Ca were the same as those shown in Figs. 1(b) and (d). The achieved high dispersibility of HAp single crystals appears to be due to the absence of the calcination-induced sintering and the cationic charge of the outermost calcium-rich surface.

In summary, calcined HAp nanocrystals were successfully prepared by calcination using an anti-sintering agent interspersed between or surrounding the particles, followed by removal of the agent. The HAp nanocrystals obtained here should be suitable for the various applications mentioned above, and also as dental and orthopedic ultrafine fillers for microporosity owing to their high dispersibility in liquid media and high thermal and chemical stability. Calcination with an anti-sintering agent has a potential application to a wide range of calcined nanoceramic powders, such as alumina, titania, and magnesia, and offer significant benefits over existing technologies because the technique is simple, inexpensive, and amenable to scale-up and processing.

Acknowledgments

We thank Dr. K. Sato of the Advanced Manufacturing Research Institute, National Institute of Advanced Industrial Science and Technology (AIST), for helpful discussions. This work was partially supported by a grant from PRESTO, Japan Science and Technology Agency, and a Research Grant for Cardiovascular Diseases from the Ministry of Health, Labour and Welfare, Japan

(1409 words)

References

1. J. FRENKEL, J. Phys. USSR 9 (1945) 385
2. G. C. KUCZYNSKI, Trans. AIME 185 (1949) 169
3. J. E. BARRALET, S.M. BEST and W. BONFIELD, J. Mat. Sci.: Mater. Med. 11 (2000) 719
4. E. LANDI, A. TAMPIERI, G. CELOTTI and S. SPRIO, J. Eur. Ceram. Soc. 20 (2000) 2377
5. D. BERNACHE-ASSOLLANT, A. ABABOUA, E. CHAMPIONA and M. HEUGHEBAERTB, J. Eur. Ceram. Soc. 23 (2003) 229
6. T. FURUZONO, K. SONODA and J. TANAKA, J. Biomed. Mater. Res. 56 (2001) 9
7. T. FURUZONO, A. KISHIDA and J. TANAKA, J.Mater. Sci.: Mater. Med. 15 (2004) 19
8. T. FURUZONO, P. WANG, A. KOREMATSU, K. MIYAZAKI, M. OIDO-MORI, Y. KOWASHI, K. OHURA, J. TANAKA and A. KISHIDA, J. Biomed. Mater. Res. B: Appl. Biomater. 65B (2003) 217
9. S. SOMIYA, K. IOKU and M. YOSHIMURA, Mater. Sci. Forum 34-36 (1988) 371
10. M. YOSHIMURA, H. SUDA, K. OKAMOTO and K. IOKU, J. Mater. Sci. 29 (1994) 3399
11. A. D. PAPARGYRIS, A. I. BOTIS and S. A. PAPARGYRI, Key Eng. Mater. 206-213 (2002) 83
12. J. E. CARLESS and A. A. FOSTER, J. Pharmaceut. Pharmacol. 18 (1966) 697
13. M. WEI, A. J. RUYS, B. K. MILTHORPE and C. C. SORRELL, J. Biomed. Mater. Res. 45 (1999) 11
14. T. FURUZONO, D. WALSH, K. SATO, K. SONODA and J. TANAKA, J. Mater. Sci. Lett. 20 (2001) 111
15. G. BONEL, J.-C. HEUGHEBAERT, M. HEUGHEBAERT, J. L. LACOUT and A. LEBUGLE, Ann. N.Y. Acad. Sci. 523 (1988) 115
16. I. R. GIBSON and W. BONFIELD, J. Biomed. Mater. Res. 59 (2002) 697
17. D. N. MISRA, J. Dent. Res. 10 (1993) 1418

18. Y. YOSHIDA, B. VAN MEERBEEK, Y. NAKAYAMA, M. YOSHIOKA, J. SNAUWAERT, Y. ABE, P. LAMBRECHTS, G. VANHERLE and M. OKAZAKI, J. Dent. Res. 80 (2001) 1565

Figure captions

Fig. 1 X-ray diffraction patterns (a, b) and FTIR spectra (c, d) of hydroxyapatite (HAp) particles calcined at 800°C for 1 h without (a, c) and with (b, d) $Ca(OH)_2$ (HAp/$Ca(OH)_2$ = 1/1 w/w) interspersed between the particles. $Ca(OH)_2$ was centrifugally washed off with an aqueous solution after calcination.

Fig. 2 SEM photographs (a, b) of HAp crystals calcined without (a) and with (b) $Ca(OH)_2$. A TEM photograph (c) and the associated electron diffraction pattern corresponding to the [210] zone (d) of a HAp crystal calcined with $Ca(OH)_2$, showing the crystal to consist of a single HAp phase.

Fig. 3 Size distributions of HAp crystals calcined without (a) and with (b) $Ca(OH)_2$. The size distributions were measured in ethanol.

Fig. 4 A SEM photograph (a) and the size distribution (b) of HAp crystals calcined at 800°C for 1 h with poly(acrylic acid calcium salt) (PAA-Ca) surrounding the particles. CaO, the product of thermal decomposition of PAA-Ca, was centrifugally washed off with an aqueous solution after calcination.

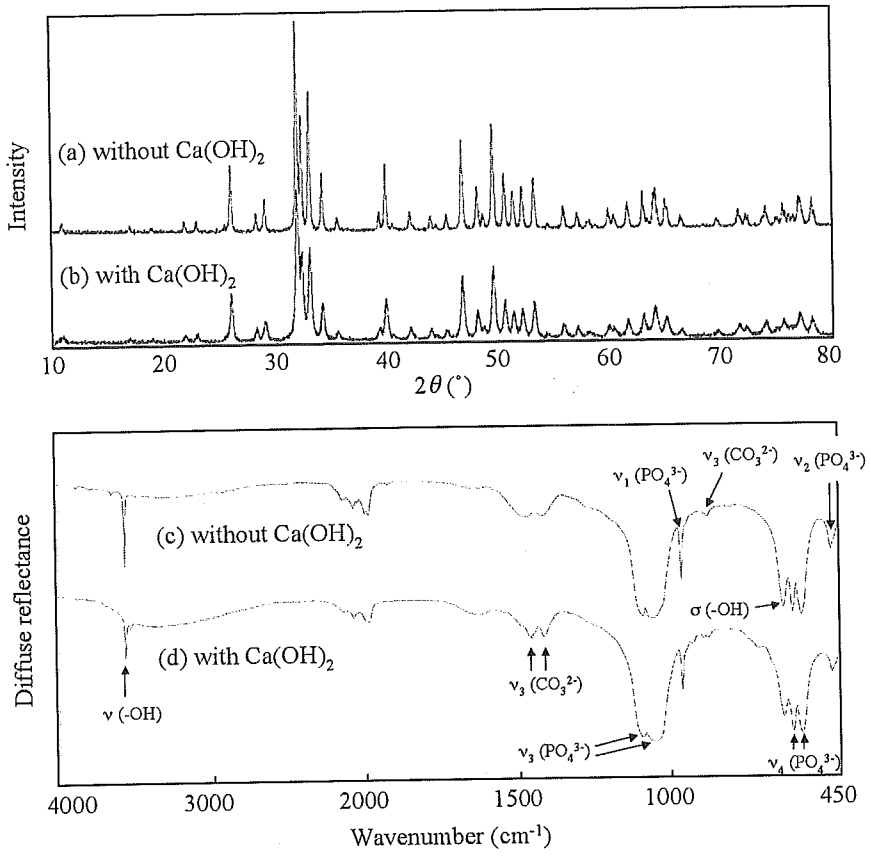

Fig. 1 Furuzono *et. al.*

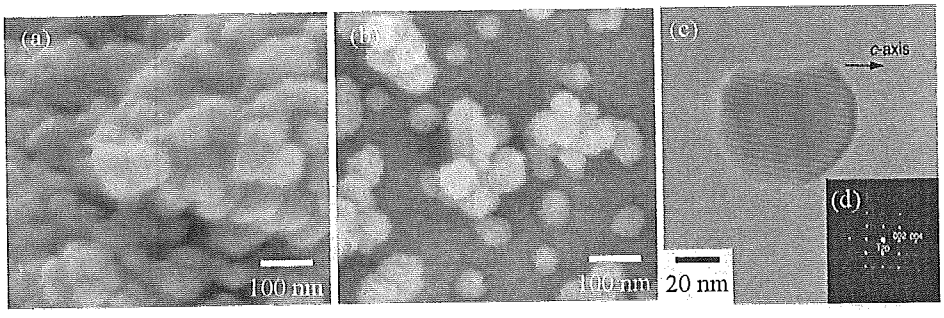

Fig. 2 Furuzono *et. al.*

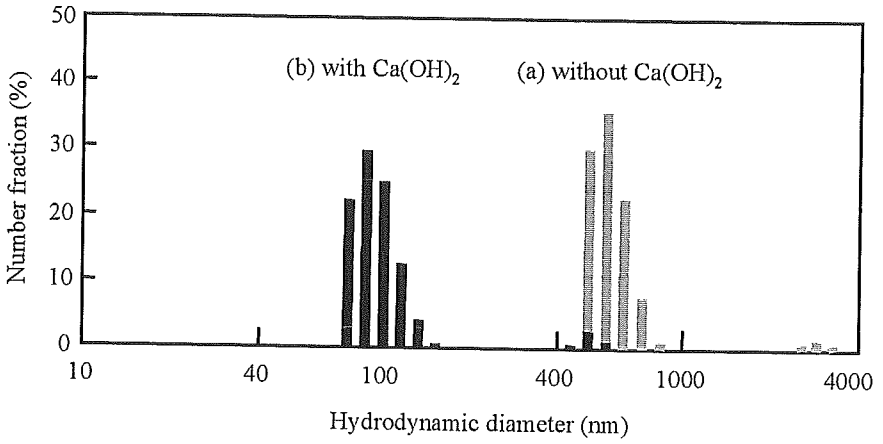

Fig. 3 Furuzono *et. al.*

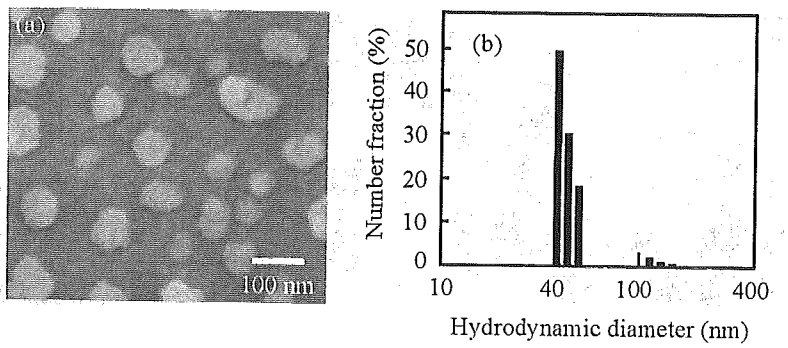

Fig. 4 Furuzono *et. al.*

J Nanoparticle Res

Highly dispersed rod-like nanocrystals of calcined hydroxyapatite fabricated by calcination with an anti-sintering agent surrounding the crystals

M. Okada[1] and T. Furuzono[1,2]

[1]Department of Bioengineering, Advanced Medical Engineering Center, National Cardiovascular Center Research Institute, 5-7-1 Fujishirodai, Suita, Osaka 565-8565, Japan

[2]Author to whom any correspondence should be addressed.

Tel: +81-6-6833-5012 (ext 2623)

Fax: +81-6-6872-7485

E-mail: furuzono@ri.ncvc.go.jp

Abstract

Sintering-free nanocrystals of calcined hydroxyapatite (HAp) having a rod-like morphology were fabricated by calcination at 800°C for 1 h with an anti-sintering agent surrounding the original HAp particles and the agent was subsequently removed after calcination. The original HAp particles having a rod-like morphology with a size ranging from 30 to 80 nm (short axis) and 300 to 500 nm (long axis) were prepared by the wet chemical process, and poly(acrylic acid, calcium salt) (PAA-Ca) was used as the anti-sintering agent. In the case of calcination without additives, the mean size of HAp crystals dispersed in an ethanol medium increased by about 4 times and the specific surface area of the crystals exhibited a 25% decrease compared to those of the original HAp particles because of calcination-induced sintering among the crystals. On the other hand, the HAp crystals calcined with the anti-sintering agent, PAA-Ca, could be dispersed in an ethanol medium at the same size as those of the original particles, and they preserved the specific surface area after calcination. These results indicate that PAA-Ca and/or its thermally decomposed product, CaO, surrounded the HAp particles and protected them against calcination-induced sintering during calcination. The HAp crystals calcined with PAA-Ca showed high crystallinity, and no other calcium phosphate phases could be detected.

1. Introduction

Hydroxyapatite (HAp, $Ca_{10}(PO_4)_6(OH)_2$) is ideal as the main mineral of bones and teeth. Artificially synthesized HAp has been extensively used in a variety of applications, such as biomaterials, ion exchangers, adsorbents, and catalysts by exploiting its biocompatibility and adsorbability with many compounds. However, owing to its mechanical weakness and brittleness [1-3], applications of HAp have been confined to those with low mechanical stress. We recently developed a novel inorganic/organic composite [4, 5]: a flexible polymer substrate, whose surface was modified with calcined HAp nanoparticles through covalent bonding. The novel composite retained the flexibility of the polymer substrate and showed HAp properties on its surface, such as tissue adhesion in a living body [6].

HAp nanoparticles can be synthesized in a number of ways, such as the wet chemical process [7-9], sol-gel process [10-12], and emulsion process [13, 14]. Among these processes, the wet chemical process has been widely used because it is simple and the morphology of the HAp particles can be changed by the reaction conditions such as pH, temperature and the concentration of the reactants or additives [7-9]. The morphology will affect the adsorption properties of biopolymers such as proteins and the ion-exchange property, because HAp belongs to a hexagonal crystal system and possesses a positive charge in its *a* plane and a negative charge in their *c* plane [15].

When low-crystallinity HAp nanoparticles synthesized *via* the above processes are calcined to increase thermal and chemical stability, the particles typically sinter into large agglomerates consisting of polycrystals [16-20]. Thus, calcined HAp crystals dispersed in a liquid medium on a nanoscale have been difficult to obtain. Hydrothermal treatment of HAp particles in an aqueous medium under high pressure is known to enable the preparation of sintering-free HAp single crystals [21-23]. However, this treatment generally leads to an increase in crystal size

due to Ostwald ripening [24, 25], and is restricted to laboratory-scale products as it is a high-pressure process.

In our previous article [26], agglomerate-free hydroxyapatite (HAp) nanocrystals having a spherical morphology were successfully fabricated by calcination with an anti-sintering agent surrounding the HAp particles and subsequent removal of the agent. That is, there was no contact among the particles during calcination. Original HAp nanoparticles with low crystallinity and a spherical morphology were prepared by a modified emulsion system [14] at 25°C, and calcined with calcium hydroxide [$Ca(OH)_2$]. $Ca(OH)_2$ was selected as the anti-sintering agent, because $Ca(OH)_2$ does not melt at the calcination temperature (800°C), presumably would not dissolve the HAp, and could be removed by washing with water after calcination.

In this article, original HAp particles having a rod-like morphology prepared by the wet chemical process were calcined with an anti-sintering agent in order to extend the application of calcination with an anti-sintering agent. Poly(acrylic acid) (PAA) was used to surround the HAp particles efficiently with the anti-sintering agent, and the thermal decomposition behavior of the agent during calcination was investigated. Furthermore, the influence of the anti-sintering agent on the crystal phase, composition, and particle size of the HAp crystals was clarified.

2. Experimental

2.1. Materials

$Ca(OH)_2$ was prepared by the hydrolysis of calcium oxide obtained by calcination of alkaline-analysis-grade calcium carbonate ($CaCO_3$; Wako Pure Chemical Industries, Ltd., Osaka, Japan) at 1050°C for 3 h. A 25% ammonia solution and diammonium hydrogenphosphate

[$(NH_4)_2HPO_4$] were purchased from Wako Pure Chemical Industries, Ltd. Guaranteed reagent-grade calcium nitrate tetrahydrate [$Ca(NO_3)_2 \cdot 4H_2O$] and ammonium nitrate [NH_4NO_3] were purchased from Nacalai Tesque Inc., Kyoto, Japan. PAA (weight-average molecular weight: 15,000), used as a polymeric stabilizer, was purchased from Sigma-Aldrich Co., MO, USA. Milli-Q water with a specific resistance of 18.2×10^6 Ω•cm was used (Millipore Corp., MA, USA).

2.2. HAp particles

Original HAp particles with a rod-like morphology were prepared by the wet chemical process as follows. 42 mM $Ca(NO_3)_2$ *aq.* and 100 mM $(NH_4)_2HPO_4$ *aq.* were prepared, and the pH of each solution was adjusted to 12.5 by adding a 25% ammonia solution. 800 mL of the $Ca(NO_3)_2$ *aq.* was poured into a 1-L reactor equipped with an inlet of N_2, a reflux condenser, and a half-moon type stirrer. After the temperature in the reactor had been raised to 80°C, 200 mL of $(NH_4)_2HPO_4$ *aq.* was added into the reactor at a feeding rate of 20 mL/h, and the resultant mixture was stirred for another 10 h at 80°C. The obtained HAp particles were centrifugally washed with water, and re-dispersed in a water medium.

2.3. Calcination

The calcination procedure of HAp particles with an anti-sintering agent is sketched in Fig. 1. An amount of PAA, approximately equal in weight to the HAp particles, was dissolved in water at 1.0 wt%, and the pH of the PAA *aq.* was adjusted to 10.0. The PAA *aq.* was added in the HAp dispersion (solid content, 1.0 wt%), and the dipsersion was ultrasonicated for 5 min. An excess amount of calcium ions was added to the dispersion in the form of a saturated $Ca(OH)_2$ *aq.* ($Ca(OH)_2$/COOH in PAA = 1/1 molar ratio) to precipitate poly(acrylic acid,

calcium salt) (PAA-Ca) onto the HAp particles. The resultant HAp/PAA-Ca mixture was filtered, dried at 80°C for 2 h under reduced pressure, and calcined at 800°C for 1 h at a heating rate of 10°C/min. Calcination was carried out in a horizontal furnace with an alumina tube in air. After calcination, the resultant powder was centrifugally washed with 100 mM NH_4NO_3 *aq.* until the pH of the dispersion decreased to almost 7.0, and then washed with water three times. As a control procedure, the same original HAp particles were calcined without adding PAA and $Ca(OH)_2$.

2.4. Thermal decomposition of PAA-Ca

PAA-Ca was precipitated by adding a saturated $Ca(OH)_2$ *aq.* into PAA *aq.* at an initial pH of 10.0 in the absence of HAp particles, and dried at 80°C for 2 h under reduced pressure. The thermal decomposition behavior of PAA-Ca was measured by a thermogravimeter (TG; EXSTAR6000 TG/DTA6300, Seiko Instruments Inc., Chiba, Japan). The heating rate was 10°C/min and the temperature range was from 30 to 1000°C.

2.5. Measurements

Identification of the product was conducted by X-ray diffraction (XRD) measurement (RAD-X; Rigaku International Co., Tokyo, Japan) with CuKa radiation, and diffuse reflectance Fourier-transform infrared (FT-IR) spectroscopy (Spectrum One; Perkin-Elmer Inc., MA. USA). The morphology of the HAp crystals was observed by scanning electron microscopy (SEM; JSM-6301F, JEOL Ltd., Tokyo, Japan) and transmission electron microscopy (TEM; JEM-2000 EXII, JEOL Ltd.). The size distribution of the HAp crystals dispersed in an ethanol medium was measured at a 10-ppm concentration by dynamic light scattering (DLS; ELS-8000, Otsuka Electronics Co., Ltd., Kyoto, Japan) at a light-scattering angle of 90°. The Ca/P atomic ratio

of each HAp was measured by inductively coupled plasma-atomic emission spectrometry (ICP-AES; SPS4000, Seiko Instrument Inc., Chiba, Japan) and X-ray photoelectron spectroscopy (XPS; PHI Model 1600S, Physical Electronics, Inc. MN, USA) at an emission angle of 45°. Calcium and phosphorus standard solutions for ICP-AES were purchased from Kanto Chemical Co., Inc., Tokyo, Japan. In the case of XPS measurements, the Ca/P ratio was calculated from the surface concentration of each atom with atomic sensitivity factor provided by Physical Electronics, Inc. The specific surface area of the particles was measured by the Brunauer-Emmett-Teller (BET) triple-point method with nitrogen adsorption (NOVA1200e, Quantachrome Instruments, FL, USA) after degassing the powder at 100°C under reduced pressure for 10 min. The data resulting from BET measurements are presented as means ± standard deviations for mean (N = 3). Statistical comparisons were performed with the use of a Student's *t* test. The level of statistical significance was defined as $p < 0.01$.

3. Results and discussion

First, in order to check the thermal decomposition behavior of PAA-Ca used as an anti-sintering agent, PAA-Ca was calcined in air at 800°C for 1 h. Fig. 2 shows the FT-IR spectra of PAA and PAA-Ca. PAA showed major peaks at 1695 cm^{-1}, corresponding to the C=O stretching of the carboxyl groups and at 1453/1415 cm^{-1}, corresponding to the CH_2 and CH bending mode of the PAA chain (Fig. 2a). In the spectrum of the PAA-Ca shown in Fig. 2b, the peak at 1695 cm^{-1} decreased and a new peak appeared at 1565/1330 cm^{-1}, corresponding to the stretching mode of ionized carboxyl groups, suggesting the formation of a significant number of Ca-O interactions [27]. These peaks disappeared after calcination of PAA-Ca (Fig. 2c) and new characteristic peaks appeared at 3644 cm^{-1}, corresponding to the OH stretching in $Ca(OH)_2$. This indicates that the organic component of PAA-Ca was completely decomposed

and PAA-Ca became $Ca(OH)_2$ after calcination. It should be noted that the formation of $Ca(OH)_2$ is favorable because it can be removed by dissolving in an aqueous medium.

The *in situ* thermal decomposition of PAA-Ca into $Ca(OH)_2$ during calcination was measured by TG as shown in Fig. 3. The TG measurement was conducted at a heating rate of 10°C/min in air. In the case of $CaCO_3$ with a calcite structure (Fig. 3a), the weight loss started at 707°C and its weight decreased by 44.2%, which is due to the detachment of CO_2 molecules (43.9% in weight, calculated from the composition of $CaCO_3$). The weight of PAA-Ca gradually decreased to 87.2% due to the evaporation of absorbed water, and drastically decreased at 516°C to 49.6% with exothermic heat, as shown in Fig. 3b. This is due to the thermal decomposition of the organic components in PAA-Ca. Another weight loss started at 683°C and 28.1% of its weight remained in the latter stage. The weight loss [(49.6-28.1)/49.6×100 = 43.3%] and the starting temperature (683°C) of the latter stage almost corresponded to those of $CaCO_3$ (weight loss, 44.2%; temperature, 707°C). These results indicate that PAA-Ca was decomposed finally into CaO with the detachment of CO_2 molecules during calcination, and $Ca(OH)_2$ was formed by a hydrolysis reaction of CaO with moisture in air, as described in the following equation:

$$PAA-Ca \xrightarrow{520°C\sim} CaCO_3 \xrightarrow{680°C\sim} CaO \xrightarrow{+H_2O} Ca(OH)_2 \quad (1)$$

The rod-like HAp particles prepared by the wet chemical process were calcined with PAA-Ca surrounding the particles (Fig. 1). In order to surround the particles with PAA-Ca, first, PAA was adsorbed on the surfaces of the HAp particles in an aqueous medium. PAA can adsorb on the HAp surfaces [28-30], and thus act as a polymeric dispersant to prevent flocculation in an aqueous medium. The addition of calcium ions into an aqueous PAA solution induces precipitation of PAA-Ca. Accordingly, when calcium ions are added to the PAA-stabilized HAp dispersion, PAA-Ca precipitates onto the surfaces of the HAp particles.

The PAA-Ca presumably acts as an anti-sintering agent, because there is no contact among the HAp particles by surrounding them with PAA-Ca and/or its thermally decomposed product, CaO, during calcination.

In order to investigate the effect of the anti-sintering agent on the crystal phase and composition of HAp, XRD and FT-IR measurements were conducted. The results are shown in Figs. 4 and 5. In Fig. 4, both the XRD profiles of the particles calcined without additives and those with PAA-Ca showed highly crystalline HAp. It is worth pointing out that no other calcium phosphate phases could be detected from either XRD profile. In the FT-IR spectra shown in Fig. 5, the absorption bands at 603/572 and 474 cm^{-1} are respectively attributed to $\nu_4PO_4^{3-}$ and $\nu_2PO_4^{3-}$ in crystalline HAp. Absorptions at 1092/1045 and 963 cm^{-1} are respectively attributed to $\nu_3PO_4^{3-}$ and $\nu_1PO_4^{3-}$. The sharp absorptions of OH stretching and vibration at 3573 and 632 cm^{-1} indicate that the material exhibits high crystallinity after the calcination (Figs. 5b-d). In the FT-IR spectrum of the HAp calcined with PAA-Ca followed by washing with water (Figs. 5c), a peak at 3644 cm^{-1} due to the stretching of OH in $Ca(OH)_2$ (observed in Fig. 5b) disappeared, suggesting complete removal of $Ca(OH)_2$. Bands at 1456/1413 and 877 cm^{-1}, attributed to CO_3^{2-}-substituted phosphate positions in the HAp lattice [31], increased in the case of calcination with PAA-Ca (Fig. 5c) as compared to that without additives (Fig. 5d). This should be due to atmospheric carbon dioxide generated by thermal decomposition of PAA-Ca during calcination. In the previous study [26], an additional band at 3544 cm^{-1} was observed after calcination with $Ca(OH)_2$, suggesting the formation of a calcium-rich apatite phase [32] on the surface layer. On the other hand, such kinds of additional bands was not clear in this study, indicating less reaction between HAp crystals and the anti-sintering agent surrounding the particles. This may be due to a smaller surface area and/or higher crystallinity of the original HAp particles prepared in this study compared with

those in the previous article.

Table 1 shows the Ca/P molar ratio of HAp crystals after calcination without and with PAA-Ca. ICP-AES detects the mean Ca/P value of the surface and inside of HAp crystals, and XPS enables surface analysis. In the case of calcination without additives, the Ca/P molar ratio measured by ICP-AES corresponded to that of stoichiometric HAp (Ca/P = 1.67), and that measured by XPS was smaller than that by ICP-AES. The difference of Ca/P between ICP-AES and XPS measurements may be due to uncertainty in the XPS measurement because of the absence of the standard sample, and/or the dissolution (or ion exchanging) of Ca ions on the surface layer, which migrated from the inside to the surface of the particles [33]. On the other hand, in the case of calcination with PAA-Ca, each Ca/P value increased as compared to that of calcination without additives, suggesting the formation of a calcium-rich apatite. The percentage of increase in the Ca/P value measured by XPS (8.6%) was larger than that by ICP-AES (3.0%), which indicates the formation of calcium-rich apatites more on the surface layers than in the inside. It is worth pointing out that the calcium-rich carbonate-substituted HAp had improved mechanical and biological properties compared to stoichiometric HAp [34]. We have already reported that the HAp nanocrystals, which were calcined with the anti-sintering agent, coated on a poly(ethylene terephthalate) (PET) substrate showed no cell toxicity and an improvement of cell adhesion, as compared to the original PET substrate [35].

Fig. 6 shows SEM and TEM photographs of the original HAp particles and the calcined HAp crystals. In the SEM photograph of the original HAp particles (Fig. 6a), they had a rod-like morphology with a size ranging from 30 to 80 nm (short axis) and 300 to 500 nm (long axis). In the case of calcination without additives, some agglomerates of micron size were observed, as shown in Fig. 6b. On the other hand, in the case of calcination with PAA-Ca, the rod-like morphology was preserved. The higher-magnification TEM image of a particle

calcined with PAA-Ca and its electron diffraction pattern (Figs. 6d and 6e, respectively) confirmed that the particle was a single HAp crystal, and the long axis of the crystal was parallel to the *c*-axis of the HAp lattice. Other calcium phosphate phases could not be detected in the inside nor on the surface layer of the HAp crystals in Fig. 6d.

The size distribution of HAp crystals and the specific surface area of the crystals are shown in Figs. 7 and 8, respectively. The size distribution shown in Fig, 7 was measured in an ethanol medium by DLS. In the case of calcination without additives, the mean size (1871 nm) and the specific surface area (15.5 m^2/g) of the crystals were respectively much larger and smaller than those of the original particles before calcination (mean size, 468 nm; specific surface area, 19.6 m^2/g), which indicate the formation of agglomerates consisting of sintered polycrystals after calcination without additives. In the case of calcination with PAA-Ca, the size distribution (mean size, 430 nm) and the specific surface area (19.6 m^2/g) of the crystals almost corresponded to those of the original particles before calcination, respectively. In addition, the size of the HAp crystals in ethanol was close to the crystallite size in the long axis (300-500 nm) determined from the electron micrographs (Fig. 6c). These results indicate that sintering between the HAp nanocrystals could be prevented by PAA-Ca surrounding the crystals prior to calcination. The achieved high dispersibility of HAp single crystals should be due to the absence of calcination-induced sintering and the cationic charge of the outermost calcium-rich surface.

4. Conclusion

HAp nanocrystals having a rod-like morphology were calcined at 800°C for 1 h with PAA-Ca used as the anti-sintering agent surrounding the particles, followed by removal of the agent. Although PAA-Ca was thermally decomposed during calcination, the decomposed

product, CaO, remained on the particle surface. In the case of calcination without additives, some large agglomerates consisting of sintered polycrystals were observed. On the other hand, the HAp nanocrystals calcined with PAA-Ca showed high dispersibility in liquid media and a large specific surface area due to the anti-sintering effect of PAA-Ca surrounding the particles. Also, the HAp crystals calcined with PAA-Ca showed highly crystallinity, and no other calcium phosphate phases could be detected. The HAp nanocrystals obtained here should be suitable for various applications, such as biomaterials, ion exchangers, adsorbents, catalysts, and dental and orthopedic ultrafine fillers for microporosity owing to their high dispersibility in liquid media and high thermal and chemical stability. Calcination with an anti-sintering agent has potential application to a wide range of calcined nanoceramic powders, such as alumina, titania and magnesia, and offer significant benefits over existing technologies because the technique is simple, inexpensive, and amenable to scaling-up and processing.

5. Acknowledgment

We thank Dr. Y. Yokogawa and Dr. K. Sato of the Advanced Manufacturing Research Institute, National Institute of Advanced Industrial Science and Technology (AIST), for helpful discussions. This work was supported by a Research Grant for Cardiovascular Diseases from the Ministry of Health, Labour and Welfare, Japan